Electronic Supplementary Information

Instantaneous one-pot synthesis of Fe-N-modified graphene as an efficient electrocatalyst for oxygen reduction reaction in acidic solutions

Kazuhide Kamiya,[†] Kazuhito Hashimoto,[†,‡,⊥,*] and Shuji Nakanishi[‡,⊥,*]

†Department of Applied Chemistry, The University of Tokyo, 7-3-1 Hongo, Bunkyo-ku, Tokyo 113-8656, Japan

‡Research Center for Advanced Science and Technology, The University of Tokyo, 1-5-3 Komaba, Meguro-ku, Tokyo 153-8904, Japan

⊥ ERATO/JST, HASHIMOTO Light Energy Conversion Project, Japan

Experimental details

(1) Synthesis of graphite oxides (GOs).

GOs were synthesized from natural graphite powder (Wako) by the modified Hummers method.[s1] Briefly, 3 g graphite powder was placed into a flask containing a solution of $NaNO_3$ (3.47 g)/concentrated H_2SO_4 (138 mL), and 12 g $KMnO_4$ was then slowly added to the solution in an ice bath. After heating the resulting mixture at 35–40 °C for 1 h with stirring, 240 mL water was added, and the solution was stirred for 30 min while the temperature was held at 90 – 100 °C. To terminate the reaction, 600 mL water was added to the flask, followed by 18 mL of a 30 wt% hydrogen peroxide solution. The synthesized GOs were washed once with a HCl solution, followed by distilled water, and was then dialyzed against ultra pure water. The GOs were dried by freeze drying.

(2) Synthesis of Fe/N-graphene, Fe-graphene and N-graphene

Five hundred and forty milligrams $FeCl_3 \cdot 6H_2O$ (2.0 mmol) and 0.69 ml pentaethylenehexamine (3.0 mmol) were dissolved in 20 ml ethanol to form Fe-Pentaethylenehexamine complexes in solution. Synthesized GO (200 mg) were dispersed in 6.1 mL of the solution containing the complexes using an ultrasonic bath, and the resulting mixture was then dried at 60 °C. The formed residue was placed at the bottom of a half-closed quartz tube, which was then filled with Ar. After filling, the tube was quickly inserted into a muffle furnace preheated to 900 °C and held for 45 s. After heat treatment, the tube was quickly removed from the furnace and cooled under Ar flow to yield Fe/N-graphene. Fe-graphene and N-graphene were prepared in the similar manner to the Fe/N-graphene except that they were obtained in

the absence of N- and Fe-sources, respectively. In addition, Fe/N-graphite were also synthesized from graphite (Wako) in the same manner to the Fe/N-graphene.

(3) Characterization of catalysts

Atomic ratios of Fe and N in Fe/N-graphene were evaluated using the integrated area of X-ray photoelectron spectra (XPS; Axis Ultra, Kratos Analytical Co.) taken with monochromated Al Kα X-rays at hν = 1486.6 eV. For detailed chemical analysis, backgrounds of core-level spectra were subtracted by the Shirley method. N 1s specta were fitted with Voigt (70% of Gaussian and 30% of Lorentzian) functions. The phase composition of Fe/N-graphene was analyzed by X-Ray diffraction (XRD; SmartLab, Rigaku). The structure of doped graphene was observed under Transmission electron microscopic (TEM; H-9000UHR, Hitachi High-Technologies Co., 300kV) and atomic force microscopy (AFM; S-image/NanoNavi Station, SII NanoTechnology Inc.). Raman spectra were recorded using a CCD array detector (Pixis 100B, Princeton Instruments) equipped with a 532-nm diode laser.

(4) Electrochemical measurements

The electrochemical activities for the ORR were evaluated using a rotating disk electrode (RDE) technique. Working electrodes were first prepared by dispersing 5 mg of doped graphene powder in 175 μL ethanol and 47.5 μL Nafion solution (5 wt% solution in a mixture of lower aliphatic alcohols and water; Aldrich). The resulting mixture was then ultrasonicated for 30 min to give the catalyst inks. A 7-μL aliquot of ink was dropped onto a glassy carbon electrode (0.196 cm^{-2}). The catalyst loading was controlled to be 0.8 mg cm^{-2}. A platinum wire and Ag/AgCl/KCl sat. were used as the counter and reference electrodes, respectively. Current densities were calculated by using the geometrical surface area of the electrode(0.196 cm^{-2}).

The number of electrons transferred per oxygen molecule was estimated from the Levich equation (1).

$$j = 0.62nFCD^{2/3}\omega^{1/2}v^{-1/6} \tag{1}$$

where j is current density, n is the number of electrons, ω is the rotational speed, F is the Faradic constant (96485 C mol^{-1}), C is the bulk concentration of oxygen ($1.13 \times 10^{-6} \text{ mol cm}^{-1}$), D is the diffusion coefficient of oxygen ($1.8 \times 10^{-5} \text{ cm}^2 \text{ s}^{-1}$), and v is the viscosity of the electrolyte ($0.01 \text{ cm}^2 \text{ s}^{-1}$).
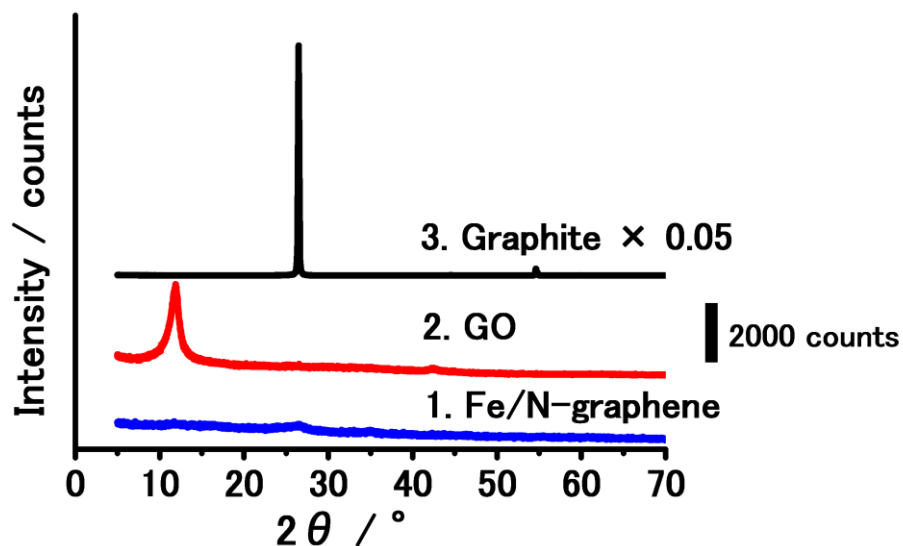
s2

Fig. S1 XRD patterns of Fe/N-graphene (curve 1), GO (curve 2), and graphite (curve 3)

The peak at around $2\theta = 12°$ for GO, corresponding to an interlayer separation of 0.7 nm, was lost after the 45 s heat treatment, implying that the graphene sheets were exfoliated.[s3-s5] In contrast, the peak corresponding to the (002) graphite interlayer spacing (0.34 nm) at $2\theta = 26.5°$ did not largely grow. These results indicate that graphene sheets exfoliated from the bulk GOs remain un-stacked after the heat treatment. It is known that rapid heat treatment increases the interlayer pressure through the evolution of gaseous CO_2 and H_2O from GOs, resulting in the exfoliation of graphene sheets.[s4,s5] Our present XRD results indicate that the same processes proceed even in the presence of Fe- and N-compounds.
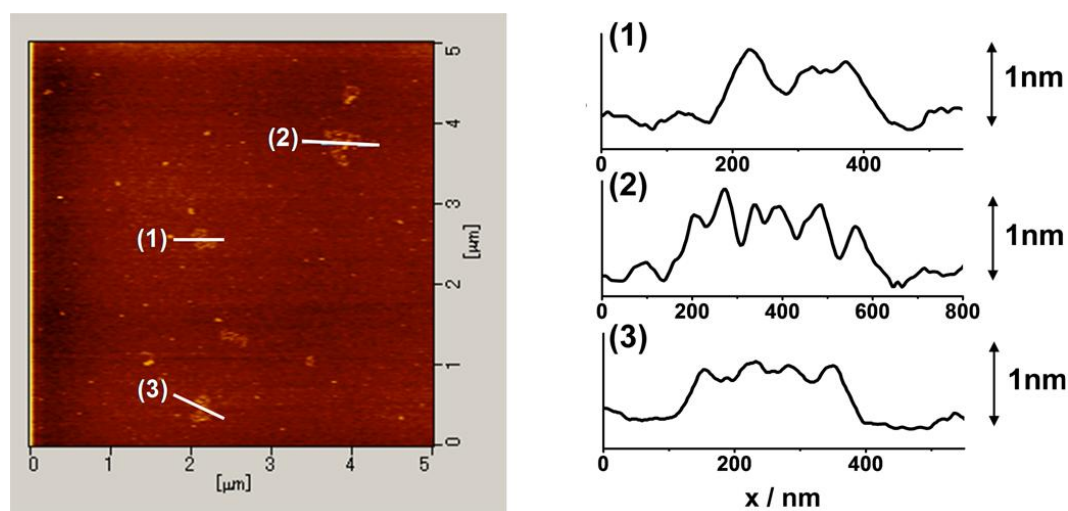
Fig. S2 Representative AFM image of the Fe/N-graphene supported on Si substrate and the corresponding height profiles along the lines marked in the AFM image. The thickness was about 1 nm, indicating the single-layer feature of the Fe/N-graphene we prepared.[s6]
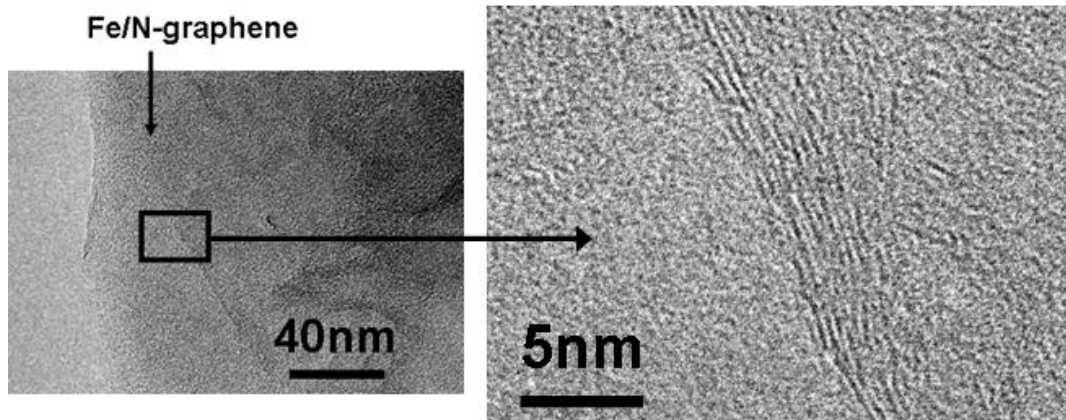

Fig. S3 Representative high-magnified TEM image (right) of Fe/N-graphene at the square region of the lower-magnified image (left).

Nanoparticles in the size of more than 1 nm cannot be observed even in the magnified TEM image, contrary to the reported carbon-based ORR catalysts prepared by conventional pyrolysis method (Ref. 1 in the main text).
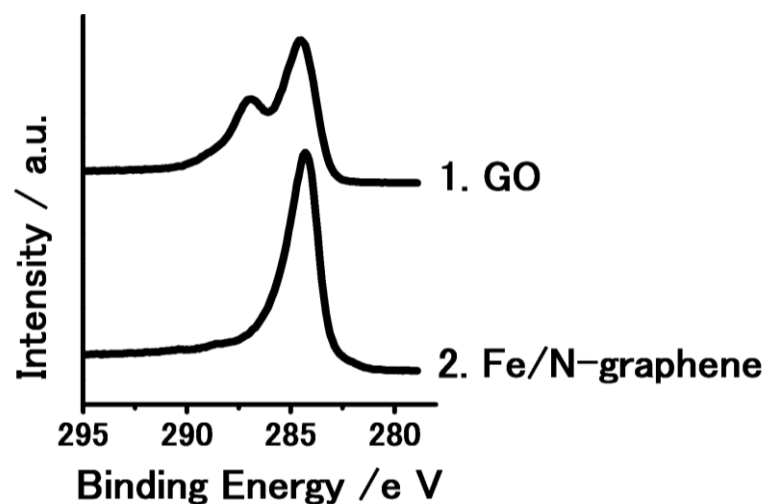
Fig. S4 XPS spectra of C 1s for GO (curve 1) and Fe/N-graphene (curve 2)

For GO, the region around C-1s exhibited an intense peak at 287 eV corresponding to C-O. For Fe/N-graphene, however, the peak at 287 eV drastically decreased and a second peak corresponding to sp2-carbon appeared at 285 eV, indicating that the GOs were reduced[s3,s4]. The thermal reduction of GO without reducing agent is considered as the result of disproportionation reaction.[s7,s8] Some of partially oxidized carbon atoms in GO are further oxidized to CO_2 or CO gases and the rest are simultaneously reduced. Thus, the reduction proceeded by thermal treatment even without additional reducing agents.
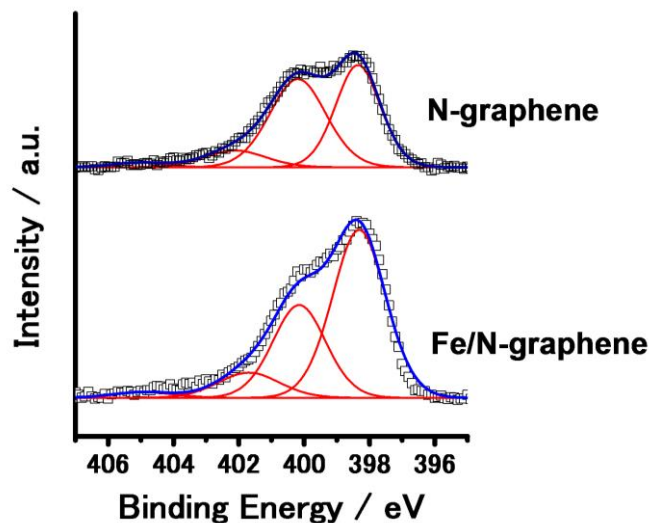

Fig. S5 XPS spectra of N 1s for N-graphene (upper) and Fe/N-graphene (lower). Black dots, measured data; blue line, fitted curve; red lines, deconvoluted curves.

Table S1 Binding energies and relative ratios of the four nitrogen components derived from decomposed N 1s XPS spectra. The assignment of each nitrogen species are described in the main text.

Fe/N-graphene	(1) N	(2) N	(3) N	(4) N
Binding Energy / eV	398.3	400.1	401.7	404.9
Relative ratio / %	57.6	31.8	8.7	2.0

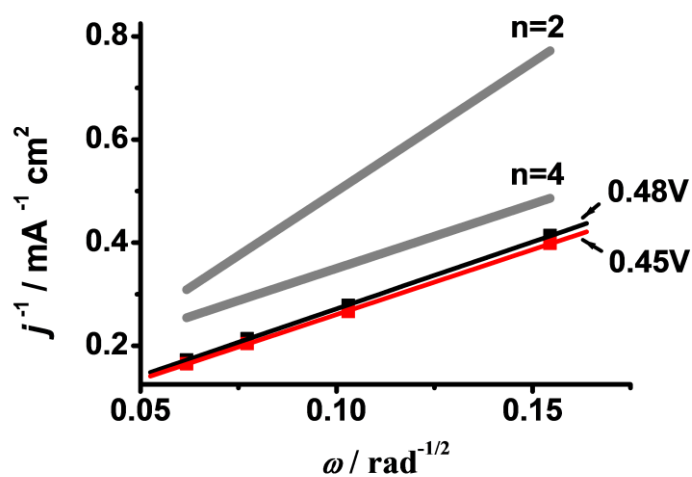| N-graphene	(1) N	(2) N	(3) N	(4) N
Binding Energy / eV	398.4	400.3	402.5	405.0
Relative ratio / %	50.0	40.4	7.4	2.2

Fig. S6 Koutecky–Levich plots at 0.48 V (black) and 0.45 V (red) vs. RHE. For comparison, the theoretical slopes (gray line) for the ORR with two- and four-electron transfers are also shown.
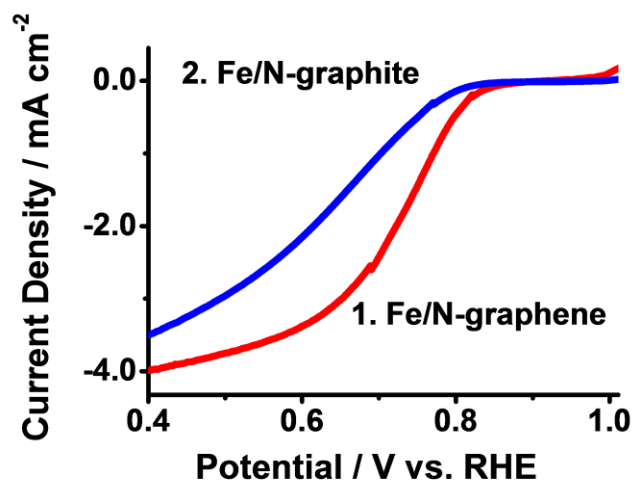
Fig. S7 j vs. U curves for Fe/N-graphene (curve 1) and Fe/N-graphite (curve 2) in 0.5 M H_2SO_4 saturated with dissolved oxygen obtained at a scan rate of 10 mV s^{-1}. Rotation speed, 1500 rpm.
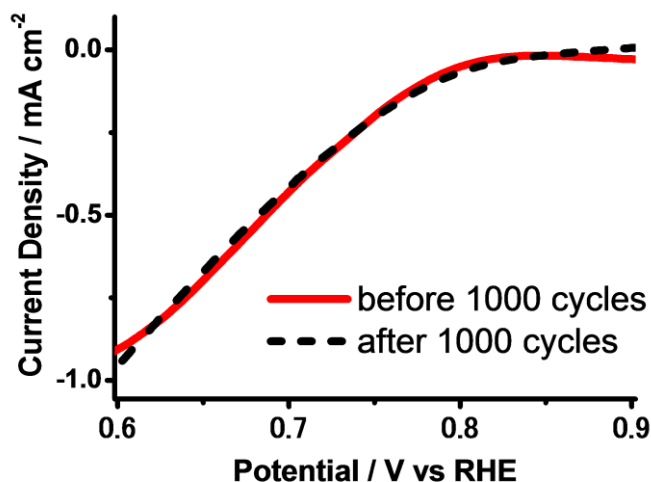

Fig. S8 j vs. U curves for Fe/N-graphene before (red) and after (black) 1000 cycles of the CVs in 0.5 M H_2SO_4 saturated with dissolved oxygen obtained at a scan rate of 10 mV s^{-1} and a rotation speed of 1500 rpm. The CV cycles were conducted at a scan rate of 200 mV s^{-1} without the rotation of electrode. The catalyst loading was controlled to be 0.2 mg cm^{-2}.
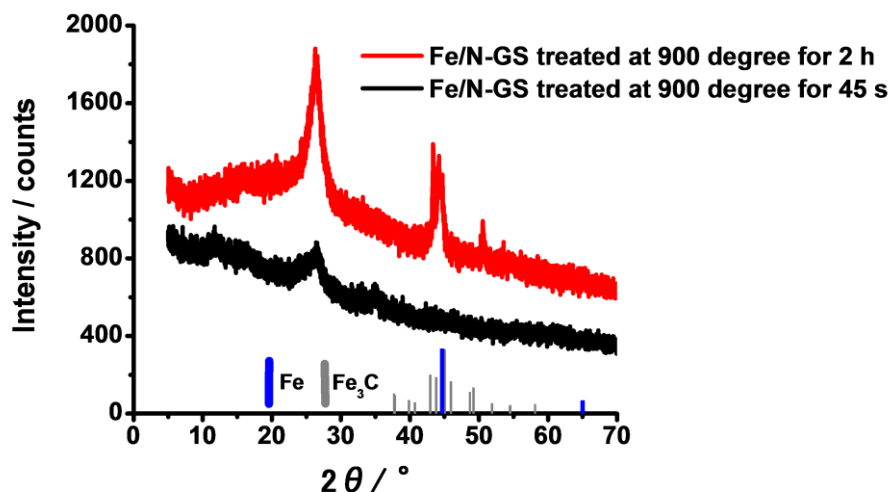
Fig. S9 XRD patterns for Fe/N-graphene heat treated for 2 h (red) and 45 s (black).

When the period of heat treatment was longer than 2 h, the peak corresponding to (002) graphite interlayer spacing (0.34 nm) at 26.5° markedly increased (red), implying that the re-stacking of graphene sheets proceeded and the effective surface area decreased during the long-duration heat treatment. Furthermore, peaks at around 44°, corresponding to iron metals and iron carbides, also appeared following the long-duration heat treatment.
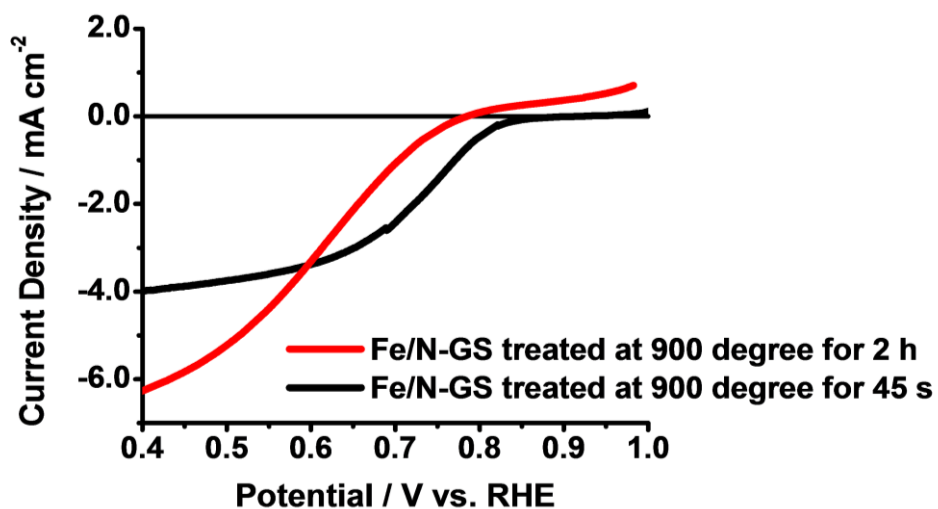

Fig. S10 j vs. U curves for Fe/N-graphene heat-treated for 2 h (red) and 45 s (black) in 0.5 M H_2SO_4 (pH = 0.33) saturated with dissolved oxygen at a scan rate of 10 mV s^{-1}. Rotation speed, 1500 rpm. The onset potential exhibited negative shift by increasing the period of the heat-treatment. Higher limiting current for the sample treated for 2h can be because of the increase of the roughness of the electrode area in the

micro-meter scale (Re-stacking and aggregation of the graphene-sheets proceed during the heat-treatment, resulting in the increase in the primary particle sizes).

Supplementary notes and references

s1. L. J. Cote, F. Kim and J. X. Huang, *J. Am. Chem. Soc.*, 2009, **131**, 1043.

s2. N. Alexeyeva, T. Laaksonen, K. Kontturi, F. Mirkhalaf, D. J. Schiffrin and K. Tammeveski, *Electrochem. Comm.,* 2006, **8**, 1475.

s3. D. Cai and M. Song, *J. Mater. Chem.*, 2007, **17**, 3678.

s4. H. C. Schniepp, J. L. Li, M. J. McAllister, H. Sai, M. Herrera-Alonso, D. H. Adamson, R. K. Prud'homme, R. Car, D. A. Saville and I. A. Aksay, *J. Phys. Chem. B*, 2006, **110**, 8535.

s5. M. J. McAllister, J.-L. Li, D. H. Adamson, H. C. Schniepp, A. A. Abdala, J. Liu, M. Herrera-Alonso, D. L. Milius, R. Car, R. K. Prud'homme and I. A. Aksay, *Chem. Mater.,*2007, **19**, 4396.

s6. S. R. Wang, Y. Zhang, N. Abidi and L. Cabrales, *Langmuir*, 2009, **25**, 11078.

s7. D. Krishnan, F. Kim, J. Y. Luo, R. Cruz-Silva, L. J. Cote, H. D. Jang and J. X. Huang, *Nano Today*, 2012, **7**, 137.

s8. Z. L. Wang, D. Xu, Y. Huang, Z. Wu, L. M. Wang and X. B. Zhang, *Chem. Commun.*, 2012, **48**, 976.

s9. H. R. Byon, J. Suntivich and Y. Shao-Horn, *Chem. Mater.*, 2011, **23**, 3421. (Ref. 4 in the main text)

Although GOs were used as the precursor in ref. 4, we excluded the catalyst reported in this paper from the "graphene-based catalysts" for the following reason. In ref. 4, g-C_3N_4 polymer was used as the N source. Due to the large molecular weight of g-C_3N_4, long-duration heat treatment was conducted for N-doping via the thermal decomposition of g-C_3N_4 polymer, despite using GO as the starting material. As a result, metallic nanoparticles were formed (Figure S3c and d in ref. 4) and the sheet-like structures of GOs were not maintained (Figure S3a in ref. 4), contrary to our Fe/N-graphene catalyst. Therefore, the catalyst reported in ref. 4 cannot be distinguished from general carbon-based catalysts prepared by the pyrolysis of nitrogen-containing polymers.